Journal of Alloys and Compounds 682 (2016) 352–356

Contents lists available at ScienceDirect

Journal of Alloys and Compounds

journal homepage: http://www.elsevier.com/locate/jalcom

Both oxygen vacancies defects and porosity facilitated NO_2 gas sensing response in 2D ZnO nanowalls at room temperature

Lingmin Yu*, Fen Guo, Sheng Liu, Bing Yang, Yanxing Jiang, Lijun Qi, Xinhui Fan

School of Materials and Chemical Engineering, Xi'an Technological University, No. 2 Xuefu Road, 710021, China

ARTICLE INFO

Article history:
Received 21 March 2016
Received in revised form
5 May 2016
Accepted 6 May 2016
Available online 9 May 2016

Keywords:
Surface defects
Porosity
ZnO nanowalls
NO_2
Gas sensing

ABSTRACT

In this report, NO_2 gas sensing properties of ZnO nanowalls fabricated by facial solution method under subsequent various annealing temperatures ranging from 350 °C to 750 °C in air have been investigated. Upon annealing in air, significant porosity and oxygen vacancies modification of the ZnO nanowalls has been observed through SEM and photoluminescence spectroscopy. The gas sensing behaviors of the fabricated sensors are systematically investigated. The ZnO nanowalls annealed at 450 °C exhibit excellent NO_2 gas response magnitude and fast response and recovery time (23 s, 11 s) at room temperature. The results reveal that, for their good sensing properties, there is a delicate balance between oxygen vacancies defects and porosity dependent on the annealing temperature.

1. Introduction

Nitrogen dioxide (NO_2) is a poisonous and corrosive gas, which is produced through combustion chemical plants and automobiles. According to the American health safety standards the threshold limit value (TLV) for NO_2 is 3 ppm [1–4]. Therefore, the detection and the emission control of NO_2 are thus crucial for reduction their noxious effects on environment and human health [5].

ZnO nanowalls always hold excellent chemical sensors for the detection of hazardous gases owing to its porous nanostructure with large surface area [6,7]. In addition, the gas-sensing mechanism of ZnO is surface-controlled type, one considers the defects of sensing materials as an important factor affecting the gas sensing response [8–10]. Therefore, introduction of more surface defects through annealing, is able to significantly enhance the corresponding response values at lower operating temperatures. However, Apart from this surface defects alteration, annealing also has aggravated the porosity of the ZnO nanowalls.

As far as the gas sensor application is concerned, the porosity and defects properties of the nanostructures under annealing temperatures are very essential to understand. Here, the grown 2D ZnO nanowalls under subsequent various annealing temperature ranging from 350 °C to 750 °C in air are subjected to investigate the NO_2 gas sensing properties. The point defects of ZnO nanostructures under various annealing temperature are analyzed by photoluminescence (PL) studies.

2. Experiments

2.1. Fabrication and characterization of ZnO nanowalls

The vertical standing ZnO nanowalls were fabricated by a facial solution method, as described in our previous work [6,7]. Finally, the thin film was rinsed by deionized water to remove residual salts, and dried in oven at 350 °C, 450 °C, 500 °C, 550 °C, 650 °C, 750 °C for 1 h, respectively.The morphology the samples was observed directly by using a scanning electron microscopy (SEM, FEI QAUANTA 400). For the TEM sample preparation, the ZnO nanowall films were scratched from substrates and dipped into ethanol and treated in an ultrasonic bath for 30min. Subsequently, a few drops of the resulting solution were dripped onto a Cu mesh grid and air-dried. The microstructural characterizations of the synthesized ZnO nanowalls were determined by a transmission electron microscope (TEM, JEM-2010). The photoluminescence spectra (PL) was recorded by using a luminescence spectrophotometer (LS55) with a 325 nm He–Cd laser (30 mW) as an excitation source.

* Corresponding author.
E-mail address: ylmyl@163.com (L. Yu).

http://dx.doi.org/10.1016/j.jallcom.2016.05.053
0925-8388/

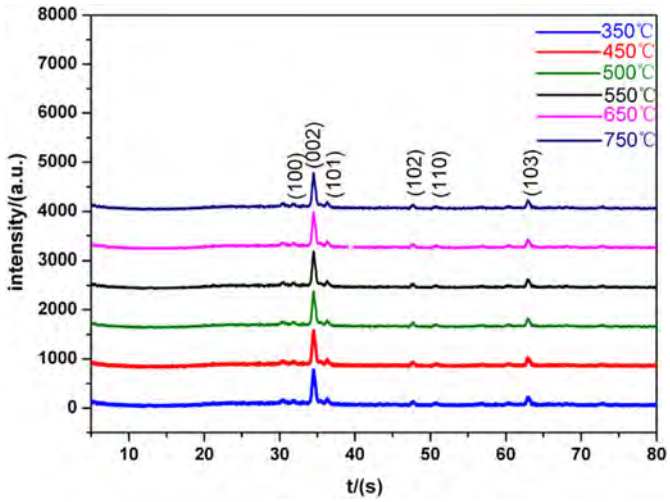

Fig. 1. XRD pattern of the product annealing at 450 °C and 750 °C.

2.2. Gas-sensing measurement

The gas-sensing properties of the sensors toward NO_2 gas were performed on a chemical gas sensor-1 Temperature Pressure (CGS-1TP) intelligent gas sensing analysis system (Beijing Elite Tech Co, Ltd.). The sensor response to an oxidizing gas was defined as the ratio of resistance of sample in the air (R_a) to its resistance in the test gas (R_g) $S = R_g/R_a$. The response time was here defined as the time required for the response to reach 90% of the equilibrium value after NO_2 was injected, and the recovery time was the time necessary for the sensor to attain a response 10% above its original value in dry air.

3. Results and discussions

3.1. Crystalline structure and morphology

The crystalstructures of the ZnO nanowalls annealed from 350 °C to 750 °C are characterized by XRD (Fig. 1). As seen in Fig. 1 a strong diffraction peak of the nanowalls appears at around $2\theta = 34.5°$, which corresponds to wurtzitestructure zinc oxide (0 0 2) peak (PDF#36–1451). However, other peaks are vary weaker, indicating that the ZnO nanowalls are well crystallized and grown along the [0 0 1] direction. In addition to that, difference in annealing temperature (350 °C–750 °C) gives little effect on the crystalline structure of the samples, and all become fully recrystallized after 1 h of annealing.

The surface topography of the as-prepared ZnO nanowalls annealed at various temperatures are elucidated by means of FESEM, as shown in Fig. 2. Fig. 2(a,b) shows the ZnO nanowalls sample annealed at 350 °C and 450 °C for 1 h, respectively. Though the diameter of porous structure composed of cross-linked walls varies from 200 nm to 500 nm, uniformly distributed nanowalls are formed and little changes in terms of ZnO nanowall structures. Further increasing the annealing temperatures (500–750 °C) yielded the microstructures shown in Fig. 2c–f, it results in remarkable alteration of the morphology, whose diameter of the most porous structure become shrunken in addition to the disappearance of some porosity which is in turn decrease the effective surface area. It is well known that the sensitivity of metal oxide semiconductor gas sensors depends on the effective surface area. These data all indicate a deterioration of the morphology quality with the decrease of effective surface area and gas sensing properties observed for the samples annealed from 500 °C to 750 °C, as mentioned below.

The as-obtained ZnO nanowall is further characterized by a typical TEM image (Fig. 3a). The sample is just composed of thin sheets and the sheets are slightly curved and interconnected each

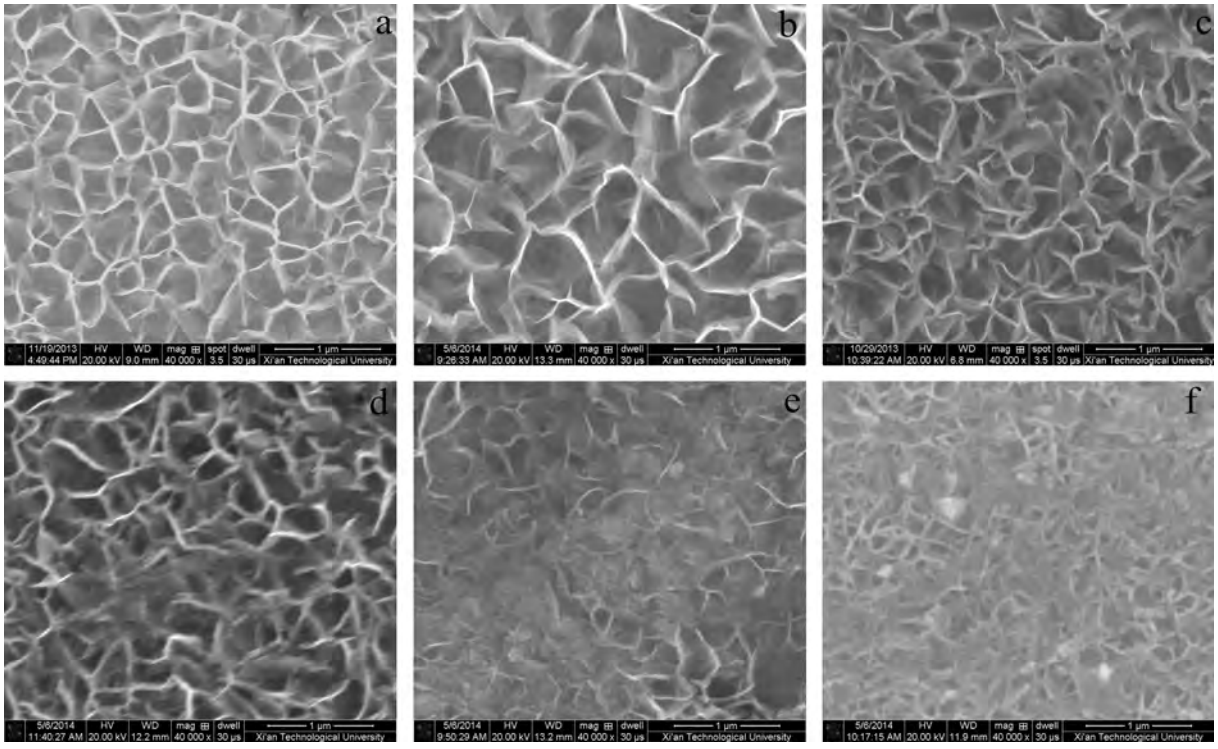

Fig. 2. The same magnification SEM images of ZnO nanowalls annealed at (a)350 °C (b)450 °C (c) 500 °C (d)550 °C (e)650 °C (f) 750 °C.

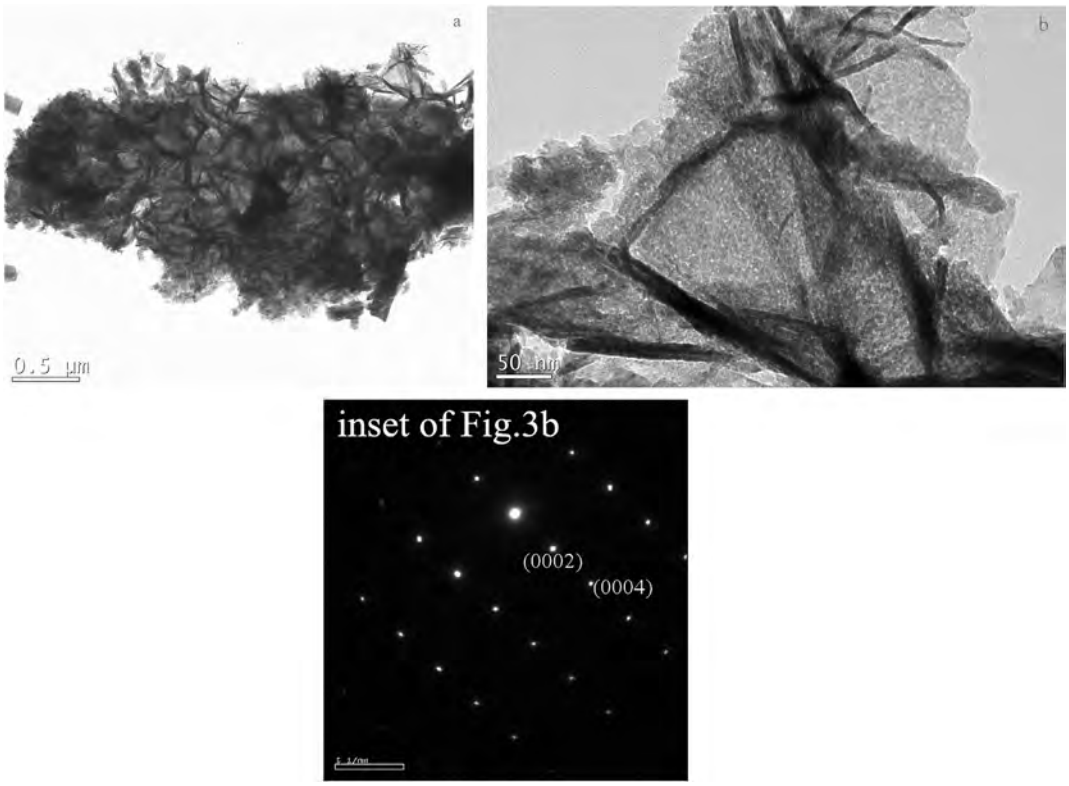

Fig. 3. Different magnification of TEM image of (a) low magnification (b) high magnification. Inset of (b) is the SEAD patterns.

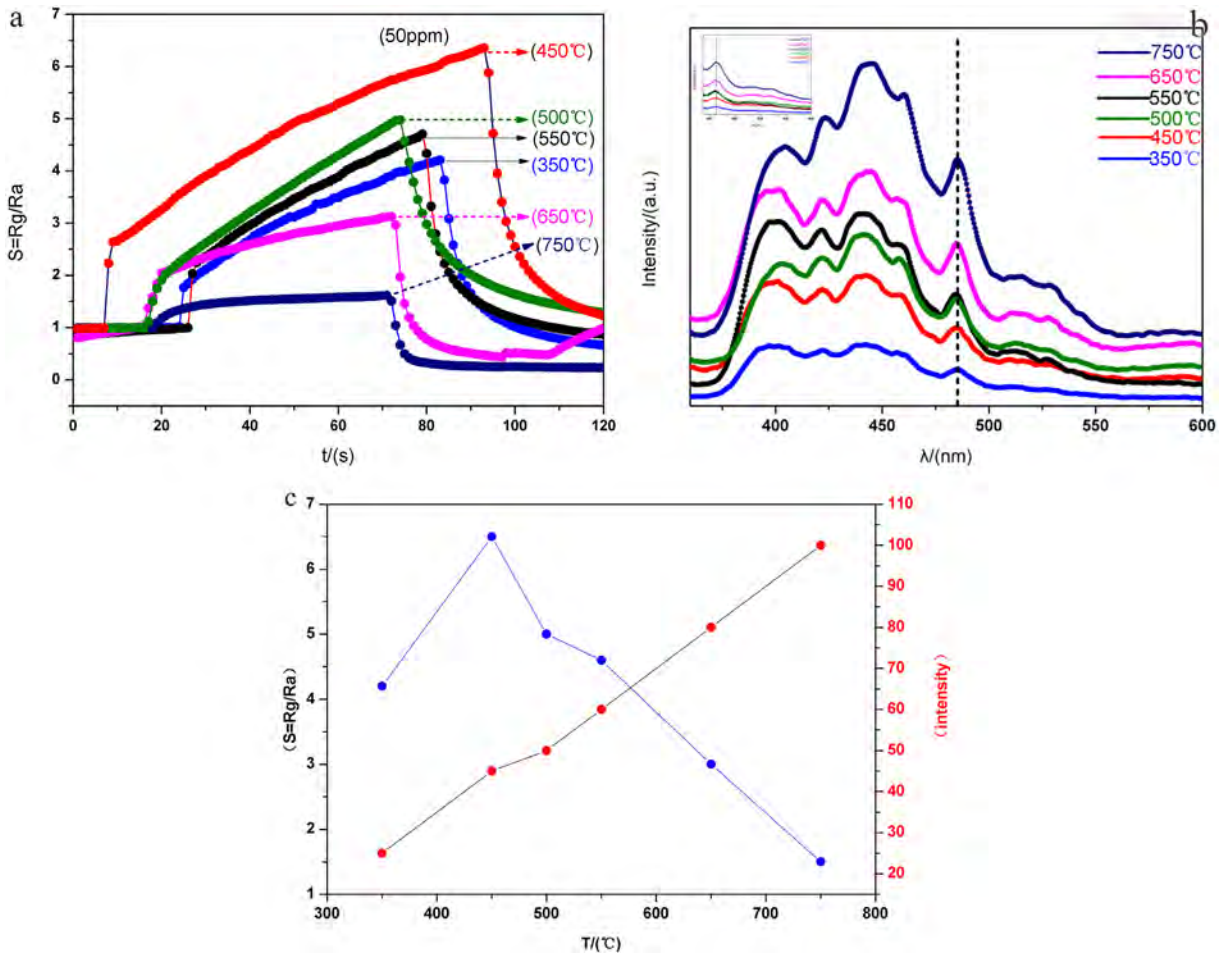

Fig. 4. (a) Typical response–recovery curves of ZnO nanowalls sensors to 50 ppm NO_2 at room temperature as a function of various annealing temperatures (b) Room temperature fluorescence emissions spectrum of ZnO nanowall samples as a function of annealing temperature. (c) relation between the oxygen vacancy defects and the gas response of ZnO nanowalls samples.

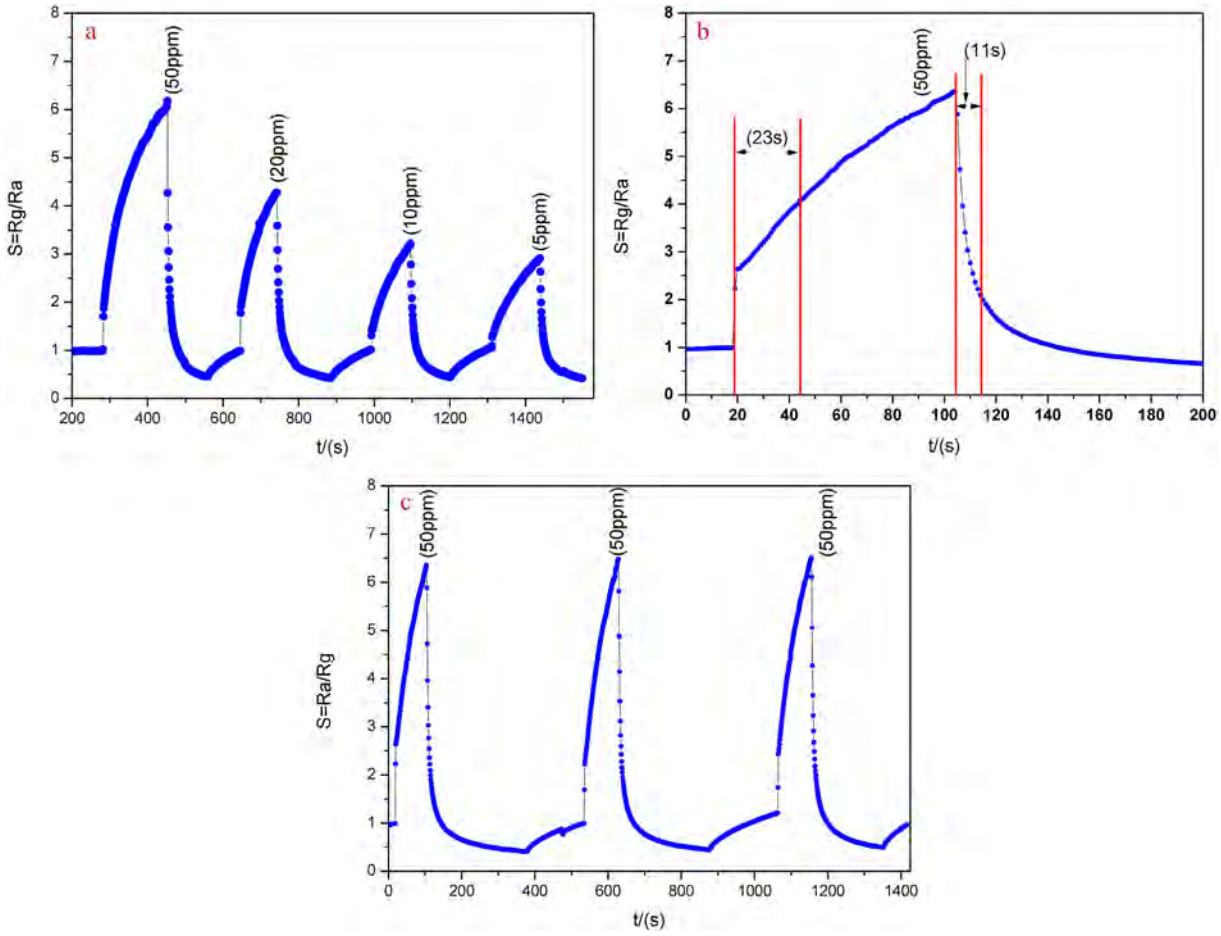

Fig. 5. (a) The response–recovery curves under exposure to NO_2 gas with different concentrations ranging from 5 to 50 ppm at room temperature. (b) one circle response transients of ZnO-450 °C gas sensors exposed to 50 ppm NO_2 at room temperature. (c) Reproducibility of temporal response of ZnO-450 °C exposed to 50 ppm NO_2 at room temperature.

other to form a porous structure. A high magnification TEM image is shown in Fig. 2b. The orientation of the ZnO nanowalls is revealed by the image contrast, where the bright and dark contrasts represent walls parallel/nearly parallel or perpendicular/nearly perpendicular to the paper surface, respectively. Apparently, the as-prepared ZnO nanowalls exhibit a triangular pore structure composed of cross-link walls with ~20 nm thicknesses (Fig. 3b). Accordingly, the SAED patterns (inset of Fig. 3b) reveal that all the diffraction dots can be well indexed to the hexagonal wurtzite ZnO structure, which grow preferentially along the [0 0 1] direction (c-axis of ZnO).

Fig. 4a shows the typical response–recovery curves of ZnO nanowalls sensors to 50 ppm NO_2 at room temperature as a function of various annealing temperatures ranging from 350 to 750 °C. It can be found clearly that the corresponding response value increases with increasing annealing temperature ranging from 350 °C to 450 °C, when the annealing temperature is beyond 450 °C (500 °C–750 °C), the gas response to NO_2 is reduced. Therefore, ZnO nanowalls annealed at 450 °C has the highest response value to NO_2 among the investigated samples. To further understand the difference response of the different gas sensors (450–750 °C), the room temperature PL spectra of ZnO nanowalls annealed at various temperature are carried out, as shown in Fig. 4 (b). The spectra have similar patterns but a considerable change in emission tensity respective of annealing temperature. The peaks at 398 and 421 nm for UV emission are originated from the recombination of free excitons. The dominant peak located at 440 nm for blue emission are attributed to the recombination between conduction band and Zn_i energy level to V_{Zn} energy level [11]. A narrow peak at 485 nm corresponds to green emission, which is attributed to the electron transition from the shallow donor level to a photo-excited hole [12,13], evidencing the presence of oxygen vacancies (V_O) in the nanostructures. The inset of Fig. 4b shows, on a magnified scale, the relative intensity deep level visible band emission as a function of annealing temperatures. These data display an increase in the relative intensity of oxygen vacancies defects in ZnO with increase of annealing temperatures. These oxygen vacancies are more beneficial for the gas sensing and that will increase the electrostatic interaction of the reactive gas molecules with the ZnO nanostructures through the surface [14]. While, the observed gas response magnitude shows no linear change with the annealing temperature that represents the oxygen vacancies defects, as shown in Fig. 4c. One observes that the maximum gas response value at 450 °C(ZnO-450 °C) whereas the oxygen vacancies defects always increases with the annealing temperature from 350 °C to 750 °C. At relatively low annealing temperatures (350 °C–450 °C), the increase in gas response to NO_2 can be correlated to the annealing led evolution of more oxygen vacancies defects on the ZnO surface but little variation in surface area. With further increase of the annealing temperature, the deterioration in the gas sensing properties may be related to the decreased porosity, which is consistent with the SEM data shown in Fig. 2. Therefore, a delicate balance between V_O defects and porosity dependent on the annealing temperature is the key factor for their good sensing

properties.

As we all known, oxygen vacancies are more beneficial for the gas sensing because it will give more electrons into the conduction band and that will increase the electrostatic interaction of the reactive NO_2 molecules with the ZnO nanostructures through the surface [14]. Hence, the width of the potential barrier decreases with an increase in V_O concentration [15].

As proposed in the following reactions (1–3), in the air ambient, oxygen molecules are adsorbed on the surfaces of ZnO nanowalls and ionized to O_2^-, by capturing free electrons from the ZnO, which directly influences the resistance of the sensor. When exposed to NO_2, the adsorbed oxygen species interact with NO_2, causing the extraction of electrons from ZnO and widening the depletion layers.

$$O_2 + e^- \leftrightarrow O_2^-(ads) \quad (1)$$

$$NO_2^-(gas) + e^- \leftrightarrow NO_2^-(ads) \quad (2)$$

$$NO_2^-(ads) + O_2^-(ads) + 2e^- \leftrightarrow NO(gas) + 2O^{2-}(ads) \quad (3)$$

To further investigate the sensing behavior of the ZnO-450 °C, the response–recovery curves under exposure to NO_2 gas with different concentrations ranging from 5 to 50 ppm at room temperature are cited in Fig. 5a. As can be seen, the overall gas sensitivity steeply increases with the increase of NO_2 concentration. The ZnO-450 °C exhibits a high response of 6.4 towards 50 ppm NO_2 at room temperature. Fig. 5b shows one circle response transients of ZnO-450 °C gas sensors exposed to 50 ppm NO_2 at room temperature, which displays the response time and recovery time are 23s and 11s, respectively. The reproducibility of temporal response of ZnO-450 °C exposed to 50 ppm NO_2 at room temperature is showed in Fig. 5c, it is seen that the sensors maintain its initial response amplitude without a clear decrease upon three successive sensing tests to 50 ppm NO_2, indicating that the sensor possesses good repeatability. All these observations confirm that ZnO-450 °C are good candidate for development of high performance NO_2 sensor operating at room temperature.

4. Conclusions

Quasi aligned ZnO nanowalls have been successfully fabricated under various annealing temperatures ranging from 350 °C to 750 °C.Among the obtained samples, ZnO-450 °C shows the best sensing response to NO_2 with fast response and recovery time and good repeatability. A combination of results from the defects and morphology analyses based on the PL and SEM characterizations suggest that both oxygen vacancies defects and porosity facilitated NO_2 gas sensing response in 2D ZnO nanowalls at room temperature. Our work is under way in our lab to further explore the gas-sensing response mechanism.

Acknowledgments

This work was financially supported by the National Natural Science Foundation of China (510721561 and 51202177) and Science & Research Fund of Education Commission of Shaanxi Province (15JK1335 and 15JK1353) and The Industrial Public Relation Project of Shaanxi Technology Committee (2016JY-206).

References

[1] Z. Huaa, Y. Wanga, H. Wang, L. Donga, NO_2 sensing properties of WO_3 varistor type gas sensor, Sens. Actuators B 150 (2010) 588–593.
[2] J. Zeng, M. Hu, W. Wang, H. Chen, Y. Qin, NO_2 sensing properties of porous WO_3 gas sensor based on anodized sputtered tungsten thin film, Sens. Actuators B 161 (2012) 447–452.
[3] L.G. Teoh, Y.M. Hon, J. Shieh, W.H. Lai, M.H. Hon, Sensitivity properties of a novel NO_2 gas sensor based on mesoporous WO_3 thin film, Sens. Actuators B 96 (2003) 219–225.
[4] A. Maity, S.B. Majumder, NO_2 sensing and selectivity characteristics of tungsten oxide thin films, Sens. Actuators B 206 (2015) 423–429.
[5] N. Tamaekong, et al., NO_2 sensing properties of flame-made MnO_x-loaded ZnO-nanoparticle thick film, Sens. Actuators B 204 (2014) 239–249.
[6] Ling-min Yu, Fen Guo, Zong-yuan Liu, Sheng Liu, Bing Yang, Ming-Li Yin, Xinhui Fan, Facile synthesis of three dimensional porous ZnO films with mesoporous walls and gas sensing properties, Mater. Charact. 112 (2016) 224–228.
[7] Lingmin Yu, Jiansong Wei, Yuyang Luo, Yanlong Tao, Man Lei, Xinhui Fan, Wen Yan, Peng Peng, Dependence of Al^{3+} on the growth mechanism of vertical standing ZnO nanowalls and their NO_2 gas sensing properties, Sens. Actuators B 204 (2014) 96–101.
[8] M. Egashira, Y. Shimizu, Y. Takao, S. Sako, Variations in I–V characteristics of oxide semiconductors induced by oxidizing gases, Sens. Actuators B 35 (1996) 62–67.
[9] Faying Fan, Yongjun Feng, Shouli Bai, Junting Feng, Aifan Chen, Dianqing Li, Synthesis and gas sensing properties to NO_2 of ZnO nanoparticles, Sens. Actuators B 185 (2013) 377–382.
[10] Lexi Zhang, Yanyan Yin, Large-scale synthesis of flower-like ZnO nanorods via a wet-chemical route and the defect-enhanced ethanol-sensing properties, Sens. Actuators B 183 (2013) 110–116.
[11] Sayan Bayan, Purushottam Chakraborty, Secondary ion mass spectrometry and photoluminescence study on microstructural characteristics of chemically synthesized ZnO nanowalls, Appl. Surf. Sci. 303 (2014) 233–240.
[12] K. Vanheusden, C. Seager, W. Warren, D. Tallant, J. Voigt, Correlation between photoluminescence and oxygen vacancies in ZnO phosphors, Appl. Phys. Lett. 68 (1996) 403–405.
[13] H. Liu, F. Zeng, Y. Lin, G. Wang, F. Pan, Correlation of oxygen vacancy variations to band gap changes in epitaxial ZnO thin films, Appl. Phys. Lett. 102 (2013) 181908.
[14] M.W. Ahn, K.S. Park, J.H. Heo, J.G. Park, D.W. Kim, K.J. Choi, J.H. Lee, S.H. Hong, Gas sensing properties of defect-controlled ZnO nanowire gas sensor, Appl. Phys. Lett. 93 (2008) 263103.
[15] N. Mendoza-Agüero, Y. Kumar, S.F. Olive-Méndez, J. Campos-Alvarez, V. Agarwal, Optimization of tungsten oxide films electro-deposited on macroporous silicon for gas sensing applications: effect of annealing temperature, Ceram. Int. 40 (2014) 16603–16610.